White Rose Research Online

eprints@whiterose.ac.uk
https://eprints.whiterose.ac.uk
Universities of Leeds, Sheffield and York

Deposited via The University of Leeds.

White Rose Research Online URL for this paper:
https://eprints.whiterose.ac.uk/id/eprint/171384/

Version: Accepted Version

Article:
Yang, X, Mao, J, Poulton, SW et al. (2021) The origin of early-Paleozoic banded iron formations in NW China. Gondwana Research, 93. pp. 218-226. ISSN: 1342-937X

https://doi.org/10.1016/j.gr.2021.02.008

© 2021, Elsevier. This manuscript version is made available under the CC-BY-NC-ND 4.0 license http://creativecommons.org/licenses/by-nc-nd/4.0/.

Reuse
This article is distributed under the terms of the Creative Commons Attribution-NonCommercial-NoDerivs (CC BY-NC-ND) licence. This licence only allows you to download this work and share it with others as long as you credit the authors, but you can't change the article in any way or use it commercially. More information and the full terms of the licence here: https://creativecommons.org/licenses/

Takedown
If you consider content in White Rose Research Online to be in breach of UK law, please notify us by emailing eprints@whiterose.ac.uk including the URL of the record and the reason for the withdrawal request.

UNIVERSITY OF LEEDS
University of Sheffield
UNIVERSITY of York

Fig. 1.

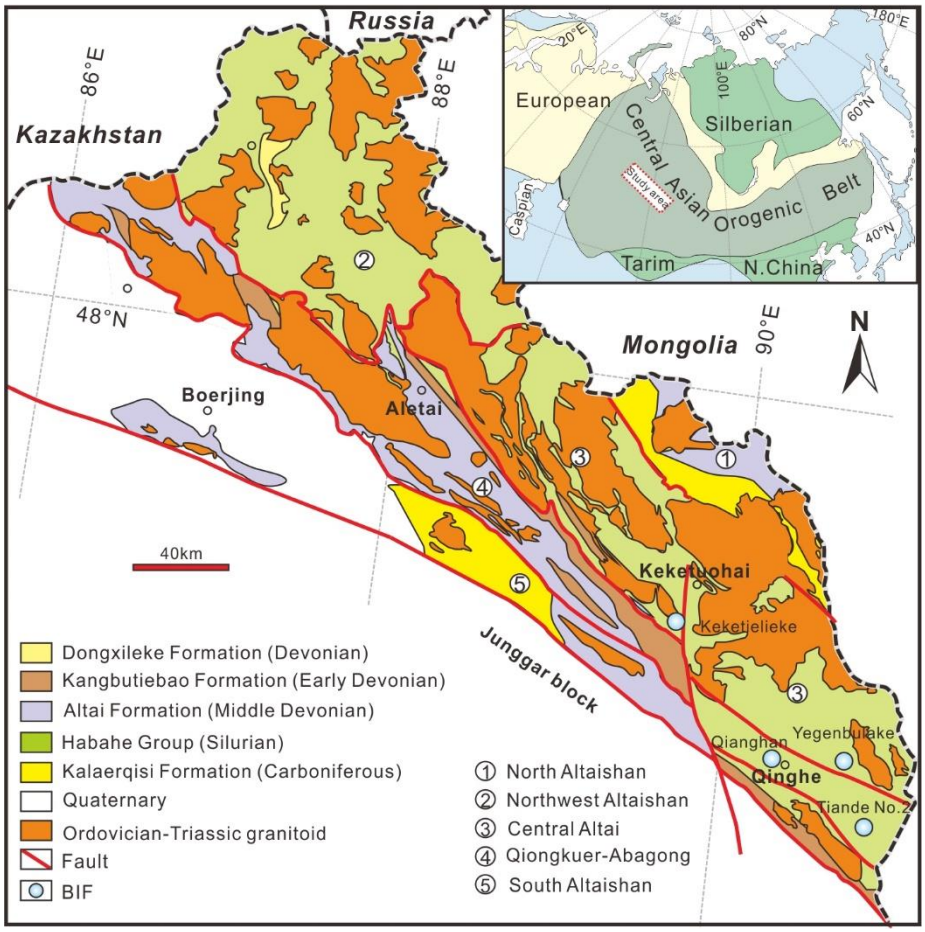
Russia
Kazakhstan
Mongolia
86°E
88°E
90°E
48°N
N
Boerjing
Aletai
40km
Keketuohai
Keketjelieke
Junggar block
Qianghan
Yegenbulake
Qinghe
Tiande No.2
Dongxileke Formation (Devonian)
Kangbutiebao Formation (Early Devonian)
Altai Formation (Middle Devonian)
Habahe Group (Silurian)
Kalaerqisi Formation (Carboniferous)
Quaternary
Ordovician-Triassic granitoid
Fault
BIF
① North Altaishan
② Northwest Altaishan
③ Central Altai
④ Qiongkuer-Abagong
⑤ South Altaishan
European
Central Asian Orogenic Belt
Silberian
Tarim
N.China
Caspian
Study area
20°E
80°N
100°E
180°E
60°N
40°N

Fig. 2.

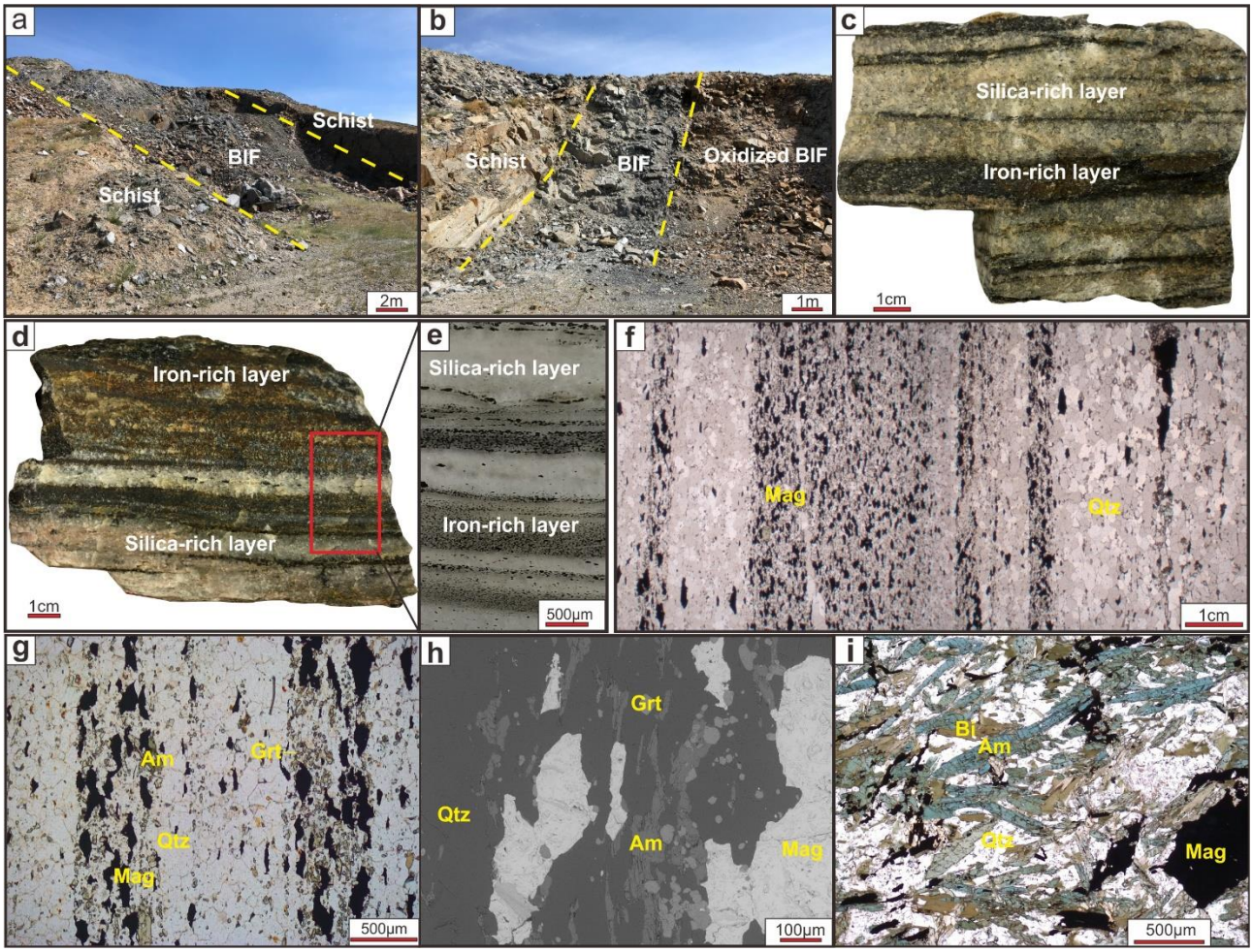
a
Schist
BIF
Schist
2m
b
Schist
BIF
Oxidized BIF
1m
c
Silica-rich layer
Iron-rich layer
1cm
d
Iron-rich layer
Silica-rich layer
1cm
e
Silica-rich layer
Iron-rich layer
500μm
f
Mag
Qtz
1cm
g
Am
Grt
Qtz
Mag
500μm
h
Grt
Qtz
Am
Mag
100μm
i
Bt
Am
Qtz
Mag
500μm

Fig. 3.

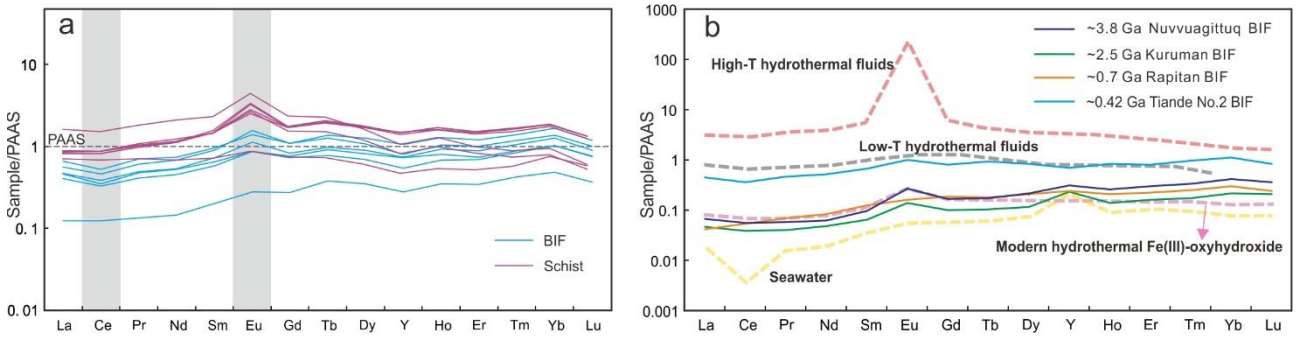
a
Sample/PAAS
PAAS
BIF
Schist
La Ce Pr Nd Sm Eu Gd Tb Dy Y Ho Er Tm Yb Lu
b
~3.8 Ga Nuvvuagittuq BIF
~2.5 Ga Kuruman BIF
~0.7 Ga Rapitan BIF
~0.42 Ga Tiande No.2 BIF
High-T hydrothermal fluids
Low-T hydrothermal fluids
Modern hydrothermal Fe(III)-oxyhydroxide
Seawater

Fig. 4.

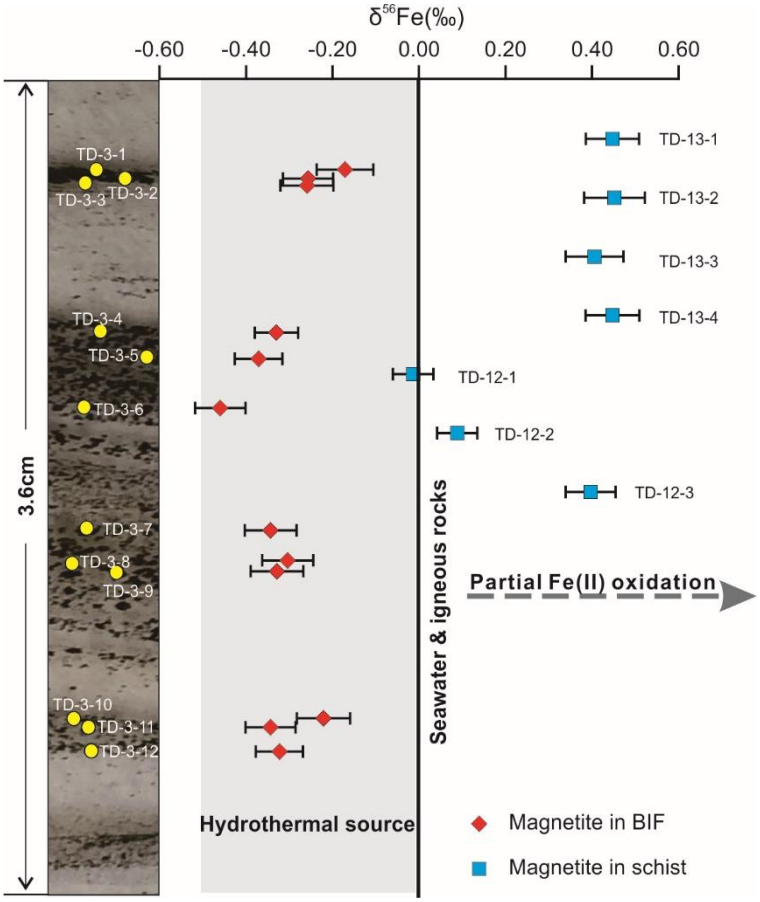
δ56Fe(‰)
-0.60
-0.40
-0.20
0.00
0.20
0.40
0.60
TD-3-1
TD-3-2
TD-3-3
TD-3-4
TD-3-5
TD-3-6
TD-3-7
TD-3-8
TD-3-9
TD-3-10
TD-3-11
TD-3-12
3.6cm
TD-13-1
TD-13-2
TD-13-3
TD-13-4
TD-12-1
TD-12-2
TD-12-3
Seawater & igneous rocks
Partial Fe(II) oxidation
Hydrothermal source
Magnetite in BIF
Magnetite in schist

Fig. 5.

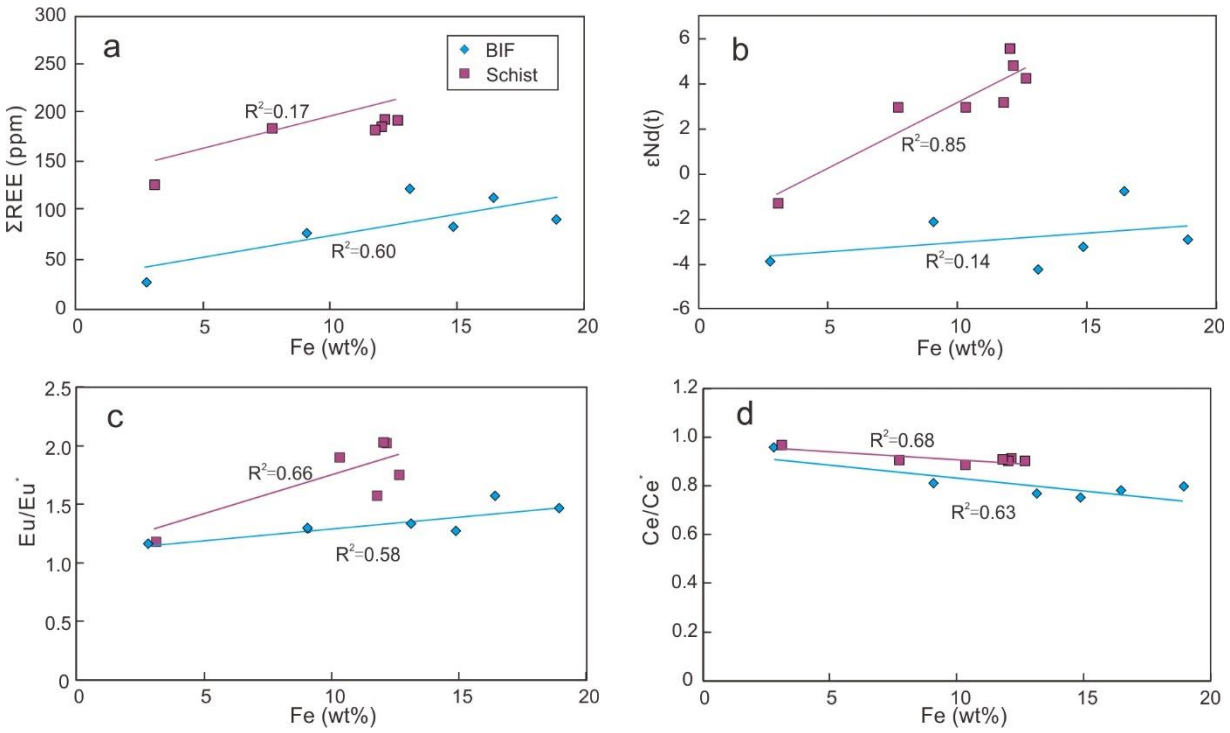
a
BIF
Schist
ΣREE (ppm)
R²=0.17
R²=0.60
Fe (wt%)
b
εNd(t)
R²=0.85
R²=0.14
Fe (wt%)
c
Eu/Eu*
R²=0.66
R²=0.58
Fe (wt%)
d
Ce/Ce*
R²=0.68
R²=0.63
Fe (wt%)

Fig. 6.

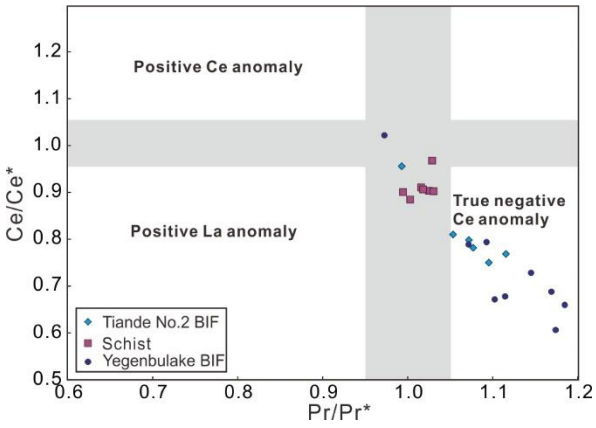
Positive Ce anomaly
Positive La anomaly
True negative
Ce anomaly
Tiande No.2 BIF
Schist
Yegenbulake BIF
Ce/Ce*
Pr/Pr*
1.2
1.1
1.0
0.9
0.8
0.7
0.6
0.5
0.6
0.7
0.8
0.9
1.0
1.1
1.2

Fig. 7.

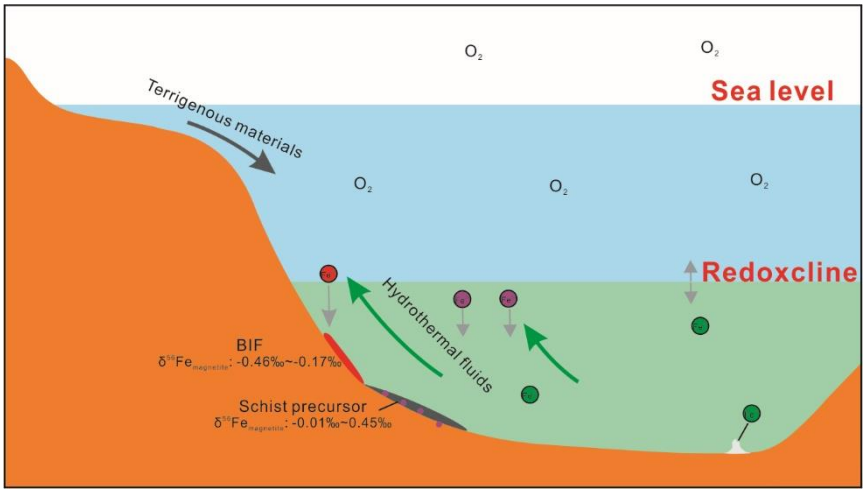
O2
O2
Sea level
Terrigenous materials
O2
O2
O2
Redoxcline
Hydrothermal fluids
BIF
δ56Femagnetite: -0.46‰~-0.17‰
Schist precursor
δ56Femagnetite: -0.01‰~0.45‰

Table 1 Nd and Fe isotopic compositions of Tiande No.2 BIF and schist samples.

Sample	Lithology	Nd(ppm)	Sm(ppm)	$^{147}Sm/^{144}Nd$	$^{143}Nd/^{144}Nd$	2σ	$\varepsilon_{Nd}(t)$	T_{DM2}(Ma)	$\delta^{56}Fe$(‰)	2σ	$\delta^{57}Fe$(‰)	2σ
TD-1	BIF	15.2	3.22	0.12807	0.512340	0.000012	-2.0	1336	-0.21	0.07	-0.31	0.09
TD-2		17.6	3.56	0.12229	0.512267	0.000009	-3.2	1426	-0.32	0.07	-0.46	0.09
TD-3		18.1	3.99	0.13327	0.512314	0.000007	-2.9	1400	-0.24	0.07	-0.35	0.08
TD-4		22.9	5	0.13200	0.512420	0.000012	-0.8	1226	-0.18	0.07	-0.30	0.08
TD-5		25	5.32	0.12865	0.512233	0.000007	-4.2	1508	-0.30	0.07	-0.44	0.08
TD-6		4.9	1.11	0.13695	0.512273	0.000006	-3.9	1481	-0.17	0.07	-0.24	0.08
TD-7	Schist	41.7	8.11	0.11758	0.512569	0.000007	3.0	926				
TD-8		71.3	12.9	0.10938	0.512547	0.000007	3.0	925				
TD-9		39.6	8.28	0.12641	0.512660	0.000019	4.2	820				
TD-10		38.7	8.72	0.13622	0.512717	0.000009	4.8	773				
TD-11		39.2	8.21	0.12662	0.512729	0.000007	5.6	712				
TD-12		23.4	4.04	0.10438	0.512316	0.000013	-1.3	1270				
TD-13		38.1	8.18	0.12980	0.512614	0.000009	3.2	909				

Note: $^{147}Sm/^{144}Nd$ are calculated using whole-rock Sm and Nd contents.

Table 2 In-situ Fe isotopic compositions of magnetite from Tiande No.2 BIF and schist samples.

Spot	Lithology	$\delta^{56}Fe$(‰)	2σ	$\delta^{57}Fe$(‰)	2σ
TD-3-01	Magnetite in BIF	-0.17	0.07	-0.26	0.12
TD-3-02		-0.26	0.06	-0.32	0.11
TD-3-03		-0.26	0.06	-0.36	0.11
TD-3-04		-0.33	0.05	-0.51	0.10
TD-3-05		-0.37	0.05	-0.53	0.11
TD-3-06		-0.46	0.06	-0.63	0.12
TD-3-07		-0.34	0.06	-0.50	0.11
TD-3-08		-0.30	0.06	-0.43	0.12
TD-3-09		-0.33	0.06	-0.47	0.12
TD-3-10		-0.22	0.06	-0.23	0.11
TD-3-11		-0.34	0.06	-0.55	0.12
TD-3-12		-0.32	0.05	-0.48	0.11
TD-13-1	Magnetite in schist	0.45	0.06	0.61	0.11
TD-13-2		0.45	0.07	0.65	0.12
TD-13-3		0.41	0.07	0.59	0.11
TD-13-4		0.45	0.06	0.69	0.11
TD-12-1		-0.01	0.05	0.01	0.09
TD-12-2		0.09	0.05	0.16	0.08
TD-12-3		0.40	0.06	0.64	0.10